GEOPHYSICS, VOL. 72, NO. 2 (MARCH-APRIL 2007); P. U21–U26, 6 FIGS.
10.1190/1.2435587

Seabed property estimation from ambient-noise recordings: Part I — Compliance and Scholte wave phase-velocity measurements

Everhard Muyzert[1]

ABSTRACT

The ability to derive a near-surface shear-velocity profile from ambient-noise records is useful for seismic applications such as shear-wave statics estimation and geohazard prediction. Measurements of seafloor compliance and Scholte wave velocity and amplitude are all related to the near-surface shear-velocity profile. I analyzed a data set of 33 minutes of continuous noise records recorded by an ocean bottom cable deployed in 273-m deep water for seafloor compliance and Scholte waves. I failed to observe seafloor compliance because of limitations in the record length. I have detected Scholte waves on the inline and vertical component geophones and Love waves on the crossline component using f-k spectra. Both the Scholte and Love wave phase-velocities can be explained by a simple 1D isotropic near-surface model. The Scholte waves may have been excited by acoustic energy from the recording vessel, while no satisfactory excitation mechanism has been found for the Love waves.

INTRODUCTION

A variety of seismic processing applications including PS-statics, wavefield separation, imaging, and geohazard prediction benefit from estimates of the near-surface shear velocity. Methods that derive a model of near-surface shear velocity reliably and efficiently are highly desirable. Direct localized measurements of near-surface shear-wave velocity can be obtained from soil samples or cone penetration tests. Such measurements are usually made at only a few locations close to the seabed. Ocean bottom seismic surveys can record the full elastic wavefield at the seafloor and allow potentially laterally continuous near-surface shear-wave estimation. Shot-generated Scholte waves propagating in the near surface have been used to estimate the near-surface shear velocity in shallow water (Muyzert et al., 2002). However, the lack of an efficient shear-wave source and the lack of PS-wave conversion for vertical incidence reflections makes near-surface shear-wave estimation a challenging task in deeper water. In this paper I study the ambient-noise field as recorded by an ocean bottom cable (OBC) and infer near-surface shear-velocity profiles from it.

Webb (1998) gives an overview of ocean bottom noise levels derived from passive ocean bottom seismometers and their sources. He divides the noise field into three distinct frequency bands; the infragravity band below 0.03 Hz, a noise notch with relatively low noise level between 0.03 and 0.1 Hz, and the short-period band near and above the microseism peak at 0.2 Hz. The noise in the infragravity band is generated by wind-driven long-period infragravity waves (sea surface waves) that propagate close to the sea surface. The noise field at frequencies between 0.1 and 5 Hz, including the microseism peak, is dominated by Scholte wave energy and generated by acoustic energy propagating in the water layer that couples into the seabed. Noise between frequencies of 5 and 10 Hz is related to wave breaking; while the spectrum between 10 and 50 Hz is dominated by man-made sources. I will focus on the noise field below 5 Hz that includes infragravity waves and the short-period band just above the microseism peak. My aim is to analyze the noise in these spectral bands and to infer near-surface properties from it.

Seafloor compliance is the inverse of sea bottom stiffness and depends on the first order of the shear modulus (e.g., Trevorrow and Yamamota, 1991; Crawford, 2000; Willoughby and Edwards, 2000). The seafloor compliance measurement is obtained by the ratio of seabed vertical displacement and water-column pressure variations that are dominated by propagating infragravity waves along the sea surface (Haubrich and McCamy, 1969; Webb, 1998). Seafloor compliance is typically measured at water depth greater than 250 m. In 250-m deep water, the compliance signal may be observed in a frequency range between 0.01 and 0.075 Hz, and is sensitive to the sediment shear modulus between 50 and 1000-m depth below the seabed (Crawford, 2000). Seafloor compliance has been inverted for shear-velocity profiles by Trevorrow and Yamamota (1991), Crawford (2000), and Willoughby and Edwards (2000).

Manuscript received by the Editor February 27, 2006; revised manuscript received October 13, 2006; published online March 1, 2007.
[1]Schlumberger Cambridge Research, Cambridge, United Kingdom. E-mail: muyzert@cambridge.oilfield.slb.com.

Scholte waves are interface waves that propagate in dispersive modes along the seabed interface. The Scholte-wave phase velocity can be measured and inverted for a near-surface shear-velocity profile of the top 100 m depending on the frequency content of data (e.g., Stoll et al., 1994; Muyzert et al., 2002). Shot-generated Scholte waves are observed usually in shallow water where the seismic source is close to the seabed. Scholte waves are not observed normally in ocean bottom seismic surveys carried out in water depths greater than 100 m. In comparison to seafloor compliance, little work has been done to infer seabed properties from Scholte waves present in the ambient-noise field. On land, Rayleigh waves, which share many characteristics with Scholte waves, have been observed in ambient-noise and its phase velocities have been measured within two-dimensional arrays (e.g., Scherbaum et al., 2003). The requirement of a two-dimensional array is a major disadvantage for seafloor applications where a small number of widely spaced one-dimensional receiver cables are deployed. The horizontal-over-vertical spectral ratio method is commonly used to estimate the near-surface shear velocity on land using microtremors and ambient-noise (Nakamura, 1989; Scherbaum, 2003). This method was first used in a marine environment by Huerta et al. (2003). This single station method assumes that the recorded data are dominated by a single noise mode.

In this paper, I analyze a 33-minute-long ambient-noise data set recorded by an OBC for seafloor compliance and Scholte waves. Using *f*-*k* spectra, I am able to identify different noise modes, I will discuss properties of the Scholte wavefield and derive a 1D model from phase-velocity measurements.

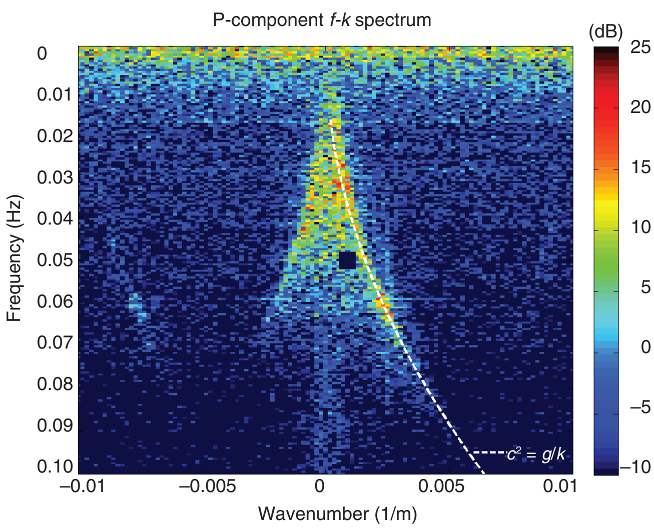

Figure 1. Frequency-wavenumber spectrum of pressure recordings. The dashed line indicates the deep water dispersion curve. The frequency range is displayed up to 0.1 Hz.

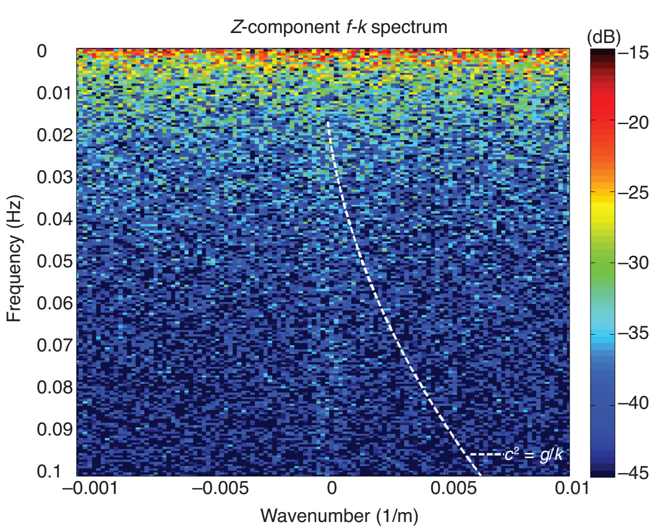

Figure 2. Frequency-wavenumber spectrum of the vertical component data.

DATA SET

The data set was collected in the North Sea, offshore Norway, at a water depth of 273 m with an OBC deployed on a sandy seafloor. The OBC had a length of 5600 m and was deployed in a straight line, it had 448 four-component receivers (pressure sensor and three-component geophones) with 12.5-m receiver spacing. The OBC's newly developed geophones had a flat response to acceleration over the seismic bandwidth and an enhanced low-frequency response compared to conventional geophones. During deployment, 33 minutes of ambient-noise were recorded at 2 ms sampling rate. A low-cut filter was not applied during data acquisition. The data were saved in 12-s long records, each having a 2-s overlap with the following record. Data preprocessing involved concatenating the 10-s unique data present in each record, followed by a decimation step, in order to reduce data volume by a factor of 25. The resulting data set, sampled at 50 ms, was used for further analysis.

SEAFLOOR COMPLIANCE

Infragravity waves, which provide the pressure force for seafloor compliance measurement, can be observed clearly in the *f*-*k* spectrum of the pressure recordings shown in Figure 1. The minimum frequency at which infragravity waves are observed is 0.01 Hz. The maximum frequency of infragravity waves is 0.06 Hz for negative wavenumbers and 0.075 Hz for positive wavenumbers; which is a result of the prevailing wave direction. The velocity c of infragravity waves closely follows the deep-water dispersion relation (Kinsman, 1983)

$$c^2 = g/k, \tag{1}$$

where g is the gravitational acceleration and k is the wavenumber. The *f*-*k* spectra for vertical and other geophone components do not show a compliance signal corresponding to the infragravity waves observed on the pressure component (Figure 2).

In the power spectral density (PSD), calculated from a pressure recording of a typical, single receiver, a peak is observed around 0.035 Hz related to the infragravity waves (Figure 3). However, the PSD for the vertical component of the geophone at the same location does not show a corresponding peak. In the compliance frequency range (0.01–0.075 Hz), the signal on the vertical component is around 120 dB below the pressure component. This is about the maximum expected compliance signal predicted by rock properties (Crawford, personal communication, 2005).

A further attempt was made to enhance the compliance signal on the vertical component through application of an *f*-*k* filter that removed energy with a lower velocity than the infragravity waves.

However, even after stacking all traces, no signal enhancement in the vertical component PSD was observed. Compliance is typically observed in much longer noise records (days instead of 33 minutes) recorded by low-frequency ocean bottom seismometers (see Crawford et al., 2005). The seabed acquisition system used in this study was not designed to record frequencies in compliance frequency range.

SCHOLTE WAVES VELOCITIES

The *f*-*k* spectra for all four components show two well-defined energy bands between 0.2 and 2.5 Hz (Figure 4). The velocity of the narrow cone of energy around zero wavenumber is about 1500 m/s and extends well above 2.5 Hz. This energy is related to acoustic waves propagating through the water layer and is not further investigated here. The lower-velocity noise cone shows dispersion, because its velocity is around 500 m/s at 0.5 Hz and 160 m/s at 2.5 Hz. The dispersion observed on the vertical, inline, and pressure

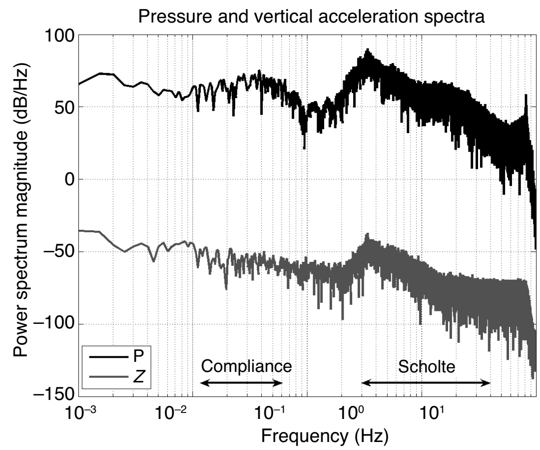

Figure 3. Power spectral density for pressure relative to 1 Pa and the vertical acceleration relative to 1 m/s^2 for receiver 100.

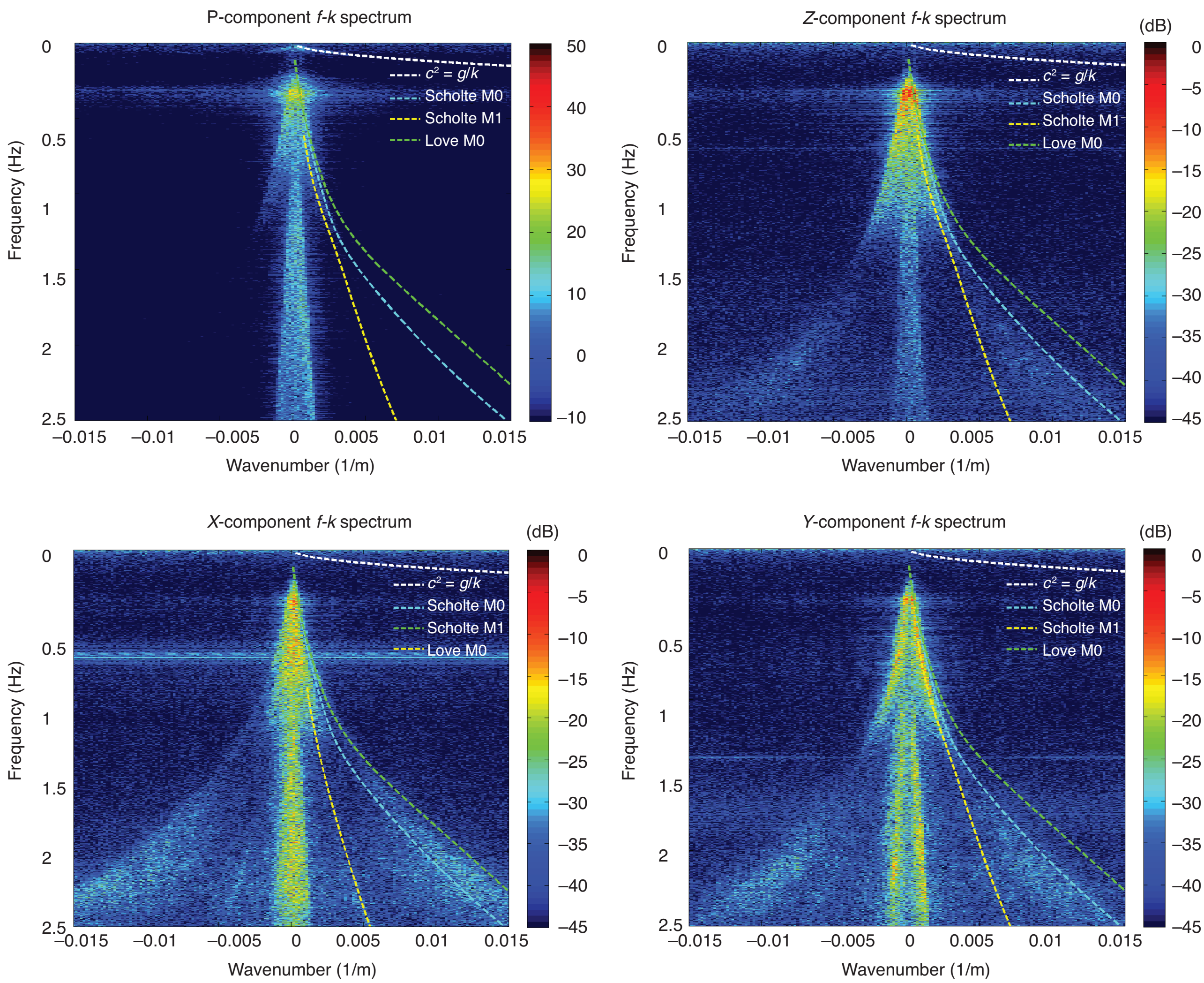

Figure 4. Calculation of *f*-*k* spectra over a record length of 33 minutes and 448 receivers. Clockwise from top left: pressure, vertical acceleration, crossline acceleration, and inline acceleration. The theoretical sea surface dispersion curve is indicated by a white dotted line, the theoretical fundamental Scholte mode (M0) by a blue dotted line, the first higher mode Scholte mode (M1) by a yellow dotted line, and Love wave dispersion curves by a green dotted line.

components is very similar; although, on the pressure component this is difficult to see because of the stronger amplitude decay for frequencies over 1.2 Hz. On the *f-k* spectrum for the crossline component, the related noise cone has about a 25% lower velocity. The noise on the vertical, inline and pressure component is interpreted as Scholte waves propagating in the near surface. The Scholte waves may propagate in any direction in the horizontal plane, depending on the azimuth of their sources with respect to the cable orientation. However, the outline of the observed band is defined by Scholte wave-energy propagating inline with the slowest apparent velocity. The radial-inline particle motion of the Scholte waves results in vertical movement of the seabed, which generates pressure waves in the water above it and is picked up by the hydrophones. The lower-velocity noise cone on the crossline component is interpreted as Love waves and will be discussed later.

PHASE-VELOCITY MODELING

Phase velocities were picked manually in the *f-k* spectra from all three geophone components. First, I discuss the inline x and vertical z component phase velocities that are nearly identical and are interpreted as Scholte waves (Figure 5). Synthetic phase velocities were calculated using the Thomson-Haskell propagator matrix method (Aki and Richards, 1980) for a number of near-surface models and compared with picked phase velocities. The first model tested was derived from shot-generated Scholte waves recorded in a more shallow part of the North Sea by Muyzert et al., (2002). The model's shear-velocity profile follows Hamilton's empirical shear-wave-velocity model for unconsolidated sediments (Hamilton, 1976). This relation is given by

$$V_S(z) = 128z^{0.28}, \tag{2}$$

where z is the depth below the sea bottom. The P-velocity and density profiles were related to the S-velocity profile through the following nonsite specific relationships. The P-velocity was related to the S-velocity profile using the mudrock line (Castagna et al., 1985):

$$V_S(z) = 0.8621V_P(z) - 1172.4. \tag{3}$$

A density profile was obtained using Gardner's (Gardner et al., 1974) relation:

$$\rho(z) = 310V_P(z)^{0.25}. \tag{4}$$

Scholte wave phase-velocities in models with a high V_P/V_S ratio, like those encountered here, are only weakly sensitive to P-velocity and density.

The overall fit between the modeled and observed phase velocity has a standard deviation of 101 m/s (Figure 5). The phase velocity for the Hamilton model is too fast for frequencies above 1.5 Hz, indicating a lower, shallow seabed velocity. The model is too slow for frequencies below 1.5 Hz and requires larger velocities at depth. By trial and error, a number of different shear-velocity models were tested against the data. A model with a constant low shear-velocity layer in the near surface was not able to fit the data satisfactorily (see the step curve in Figures 5 and 6). A model simulating a steep gradient in the near surface turned out to be very successful, as it had a 95% phase-velocity variance reduction over the Hamilton model (see the gradient curve in Figures 5 and 6).

While the vertical and inline phase velocities are almost identical, the picked crossline y component phase velocity is about 25% slower (Figure 5). Love wave phase velocities have also been calculated for the models shown in Figure 6. The Love wave data are best fitted with the same model that fits the Scholte wave data. This supports the interpretation that the inline and vertical noise field are dominated by Scholte waves and the crossline noise by Love waves.

Theoretical Scholte and Love wave phase-velocity curves for the gradient model show good agreement with the *f-k* spectra shown in Figure 4. It is evident that the event on the crossline component, associated with the Love waves, is slower and is explained well by the theoretical Love wave phase velocity. I observed a weak event on the inline component that correlates with the first higher mode Scholte wave. A similar event was observed on the crossline component that correlates with the first higher mode Love wave.

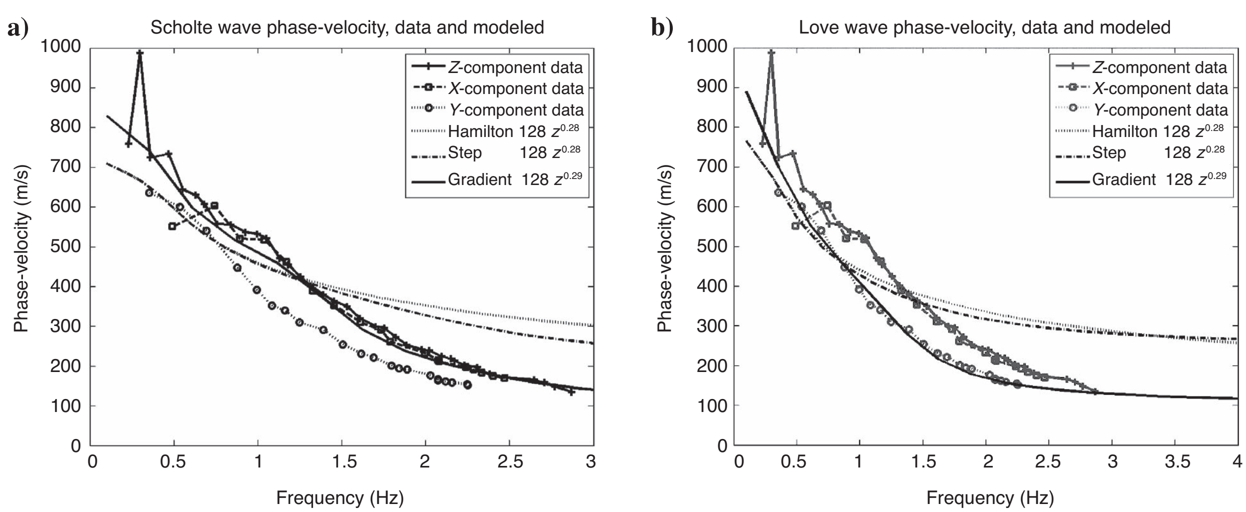

Figure 5. (a) Phase-velocity data picked in the *f-k* spectra and modeled Scholte wave phase-velocity. (b) Phase-velocity data and modeled Love wave phase-velocity.

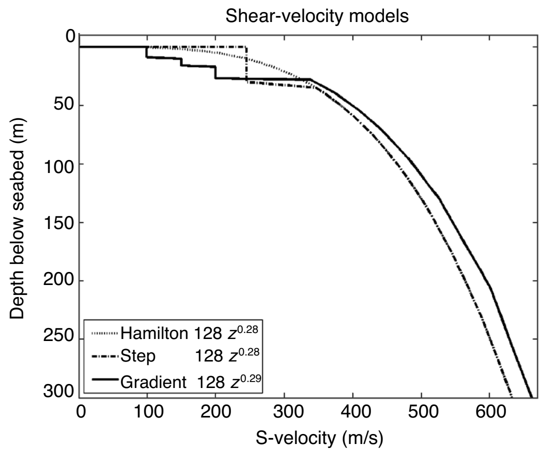

Figure 6. Models used for phase-velocity modeling.

ON THE EXCITIATION OF SCHOLTE AND LOVE WAVES

Two natural mechanisms explain the excitation of Scholte wave noise: In calm weather the interaction of wind with the sea surface waves is dominant, while in rougher weather nonlinear wave interaction becomes dominant (Kibblewhite and Wu, 1991). Nonlinear wave interaction requires waves propagating near the sea surface in opposite directions, resulting in a second-order pressure wave that converts into a Scholte wave with double the frequency as the sea-surface wave frequency. Seafloor irregularities such as slopes and rough surfaces can increase the coupling of acoustic energy into Scholte wave energy and Love waves (Rind and Donn, 1979; Liu et al., 1993; Bradley and Stephen, 1996). However, in our survey area, no significant dip has been reported and the cable's orientation of 297° does not align with the nearest coastline (Norway) that runs north and south, or with the bathymetric gradient, which is perpendicular to the east-west coastline. A sidescan performed before cable deployment did not reveal significant scatterers, thus Love wave generation through surface irregularities is also unlikely. Local Scholte-to-Love wave conversion through subsurface scattering is also unlikely, because it would require a highly scattering, possibly anisotropic, medium to result in a Love wave with similar energy as a Scholte wave energy. In that situation, some Love wave energy would also be observed on the inline component, which is not the case.

Another possible cause for the observed Love and Scholte wave directionality might be vector infidelity and imperfect coupling of the cable system with the seabed. However, this can also be ruled out because poor vector fidelity in older cable-based systems manifested itself on the crossline component as a filter with low-frequency amplification around a resonance frequency and above which it acts as a high-cut filter (Bagaini and Muyzert, 2004). This resonance frequency is typically between 20 and 40 Hz for shear waves, which is well above the frequency range of the data considered in this study. Furthermore, our data set was acquired with a new cable system and has been extensively tested for vector fidelity. A study on data shot during the same deployment sequence found excellent vector fidelity characteristics over the seismic bandwidth and all four components (Kragh et al., 2004).

A plausible explanation for the strong directionality in the Love and Scholte waves is that it was generated by the recording vessel. The recording vessel lies at one end of the cable and emits acoustic noise through its power generator, thrusters keep the vessel at a fixed position, and its controlled by the dynamic positioning system. Waterborne noise generated by the recording vessel may induce vertical motion in the seabed and convert into Scholte waves that propagate in the vertical-radial direction. More intriguing is the existence of Love waves on the crossline component. It is not understood how acoustic energy from the recording vessel will couple into Love waves. Further understanding may be acquired from a study into the vessel-generated noise field and its interaction with the seabed.

CONCLUSIONS

Analysis of the low-frequency spectrum of ambient-noise recordings on the seafloor by an OBC system has shown the existence of three dominant noise modes: infragravity waves, waterborne noise, and interface waves such as Scholte and Love waves. The infragravity waves were observed on the hydrophones, but not on the geophones. In order to observe seafloor compliance longer records are required (days instead of minutes of observation time) together with an acquisition system designed to record frequencies well below the seismic bandwidth. Waterborne noise was not discussed in this paper. Scholte waves were observed on the pressure, inline, and vertical component; while Love waves were observed on the crossline component. Modeling shows that a single 1D model with a low shear-velocity gradient zone at the top and power law relation slightly steeper than Hamilton's curve further down can explain both the observed Scholte and Love wave phase velocities. In the accompanying paper a 2D shear-velocity model of the near surface is obtained from the inversion of the spectral ratio of Scholte waves.

The water depth where the Scholte and Love waves have been observed is 273 m, well over the depth (100 m) where such waves are commonly observed in shot-generated data. Seismic applications such as converted wave statics, wavefield separation, and geohazard prediction using data acquired in deeper water may benefit from these results; there are several areas that require further research. A model of the generation of Scholte and Love wave energy in the seabed is desirable, as it will lead to a better understanding of the data and help with the planning of future acquisition, such a model should include noise generated by the recording vessel. Further experimentation is required because it is not clear at present if the observed directionality of Love and Scholte wavefields is a unique feature of the current data set or is a general feature of OBC surveys.

ACKNOWLEDGMENTS

I thank Satish Singh and Wayne Crawford for discussion on compliance measurements, and Leendert Combee, Nicolas Goujon, Ed Kragh, Robert Laws, and Karin Schalkwijk for various discussions, and Wayne Crawford, Jay Pulliam, an anonymous reviewer, and associate editor Deyan Draganov for their reviews. Data were recorded by WesternGeco Bluefin.

REFERENCES

Aki, K., and P. G. Richards, 1980, Quantitative seismology: Theory and methods: W. H. Freeman & Co.
Bagaini, C., and E. Muyzert, 2004, Calibration of cross-line components for

sea-bed 4C acquisition systems: Geophysical Prospecting, **52**, 341–349.
Bradley, C. R., and R. A. Stephen, 1996, Modeling of seafloor wave propagation and acoustic scattering in 3-D heterogeneous media: Journal of the Acoustical Society of America, **100**, 225–236.
Castagna, J. P., M. L. Batzle, and R. L. Eastwood, 1985, Relationships between compressional-wave and shear-wave velocities in clastic silicate rocks: Geophysics, **50**, 571–581.
Crawford, W., 2000, Seafloor compliance measurements: Application for hydrocarbon exploration: Lithos Science Report, **2**, 151–156.
Crawford, W., S. Singh, T. Hulme, and J. R. Smallwood, 2005, Applications of seafloor compliance measurements in the Faroes-Shetland Basin: Faroe Islands Exploration Conference, Proceedings of the 1st Conference, Annales Societatis Scientiarum Færoensis, Supplementum, **43**, 32–43.
Gardner, G. H. F., L. W. Gardner, and A. R. Gregory, 1974, Formation velocity and density—The diagnostic basis for stratigraphic traps: Geophysics **39**, 770–780.
Hamilton, E. L., 1976, Shear wave velocity versus depth in marine sediments, A review: Geophysics, **41**, 985–996.
Haubrich, R. A., and K. McCamy, 1969, Microseisms, Coastal and pelagic sources: Reviews of Geophysics, **7**, 539–571.
Huerta-Lopez, C., J. Pulliam, and Y. Nakamura, 2003, In situ evaluation of shear-wave velocities in seafloor sediments with a broadband ocean-bottom seismograph: Bulletin of the Seismological Society of America, **93**, 139–151.
Kibblewhite, A. C., and C. Y. Wu, 1991, The theoretical description of wave-wave interactions as a noise source in the oceans: Journal of the Acoustical Society of America, **89**, 2241–2251.
Kinsman, B., 1983, Wind waves, their generation and propagation on the ocean surface, 2nd ed.: Dover Publ. Inc.
Kragh, E., A. Vigner, S. Buizard, A. Stroemmen-Melboe, S. Horne, J. Robertsson, L. Combee, K. Iranpour, N. Goujon, J. Gaiser, P. Caprioli, E. Muyzert, and J. Martin, 2004, Vector fidelity characterization of a marine multi-component acquisition system: 66th Annual Conference and Exhibition, EAGE, Extended Abstracts, P293.
Liu, J.-Y., H. Schmidt, and W. A. Kuperman, 1993, Effect of a rough seabed on the spectral composition of deep ocean infrasonic ambient noise: Journal of the Acoustical Society of America, **93**, 753–769.
Muyzert, E., J. Kommedal, K. Iranpour, and B. Olofsson, 2002, Near surface S-velocities, statics and anisotropy estimated from Scholte Waves: 64th Annual Conference and Exhibition, EAGE, Extended Abstracts, F28.
Nakamura, Y., 1989, A method for the dynamic characteristics estimation of subsurface using microtremor on the ground surface: Quarterly Report of the Railroad Technical Research Institute, **30**, 25–33.
Rind, D., and W. L. Donn, 1979, Microseism at Palisades 2 — Rayleigh wave and Love wave characteristics and the geologic control of propagation: Journal of Geophysical Research, **84**, 5632–5642.
Scherbaum, F., K. G. Hinzen, and M. Ohrnberger, 2003, Determination of shallow shear velocity profiles in the Cologne, Germany area using ambient vibrations: Geophysical Journal International, **152**, 597–612.
Stoll, R. D., G. M. Bryan, and E. O. Bautista, 1994, Measuring lateral variability of sediment geoacoustic properties: Journal of the Acoustical Society of America, **96**, 427–438.
Trevorrow, M. V., and T. Yamamoto, 1991, Summary of marine sedimentary shear modulus and acoustic speed profile results using a gravity wave inversion technique: Journal of the Acoustical Society of America, **90**, 441–456.
Webb, S. C., 1998, Broadband seismology and noise under the ocean: Reviews of Geophysics, **36**, 105–142.
Willoughby, E. C., and R. N. Edwards, 2000, Shear velocities in Cascadia from seafloor compliance measurements: Geophysical Research Letters, **27**, 1021–1024.